Plasma Chem Plasma Process (2015) 35:143–157
DOI 10.1007/s11090-014-9588-3

ORIGINAL PAPER

Removal of Model Pollutants in Aqueous Solution by Gliding Arc Discharge. Part II: Modeling and Simulation Study

Iya-Sou Djakaou · Rédouane Mouffok Ghezzar · Mohamed El-Mehdi Zekri · Fatiha Abdelmalek · Simeon Cavadias · Stéphanie Ognier

Received: 19 May 2014 / Accepted: 1 October 2014 / Published online: 16 October 2014

Abstract The aim of this work is the modeling of plasma-chemical reactions taking place between highly oxidizing gaseous species ($^{\cdot}OH$, $^{\cdot}NO$ and derivatives), generated by Gliding Arc Discharge in Humid Air (GAD-HA), and organic pollutants in aqueous solution. Theses pollutants were chosen on the base of their volatility at atmospheric and ambient conditions: 1-Heptanol (highly volatile), phenol (moderately volatile) and para-chlorobenzoic acid, *p*CBA (poorly volatile). The mass transfer model of diffusion-convection was coupled to a proposed kinetic model in order to describe the phenomenology of the electrical process. The mass transfer model was obtained independently by stripping toluene and phenol molecules. The simplified kinetic model was proposed with the main reactions in gas and liquid phases mentioned in the literature. The only adjustable parameter of the model was the $^{\cdot}OH$ concentration in the plasma plume. For a concentration of $^{\cdot}OH$ of 24 ppm in the plasma plume, the model gives results in agreement with experimental results for the three model pollutants tested. The coupling of the experimental results and the simulation study allowed us to: (1) confirm that the main removal mechanism is different according to the nature of the pollutant and depends on the pollutant properties (reactivity, volatility), (2) calculate [$^{\cdot}OH$], [ONOOH] and [$NO_2^{\cdot}$]. The results of this work can be used to assist experiences in the plasma engineering field.

Keywords Gliding Arc Discharge · Modeling · Pollutants · Mechanism · $^{\cdot}OH$ · $NO_2^{\cdot}$ · HOONO

I.-S. Djakaou · R. M. Ghezzar (✉) · M. E.-M. Zekri · S. Cavadias · S. Ognier
Institut de Recherche de Chimie Paris, CNRS – Chimie ParisTech, 11 rue Pierre et Marie Curie, 75005 Paris, France
e-mail: redouane.ghezzar@chimie-paristech.fr; m.ghezzar@univ-mosta.dz; ghezzar_redouane@yahoo.fr

R. M. Ghezzar · F. Abdelmalek
Laboratoire des Sciences et Techniques de l'Environnement et de la Valorisation (STEVA), Faculté des Sciences et de la Technologie, Université de Mostaganem, BP 227, 27000 Mostaganem, Algeria

Introduction

Non thermal plasma and especially Gliding Arc Discharge are increasingly used for the treatment of organic pollutants in water. The use of the humid air as plasma-gas reduces the cost of process and permits to generate reactive species with short lifetime such as $^{\cdot}OH$ and $^{\cdot}NO$, and long lifetime such as O_3, H_2O_2, HONOO and N_2O_4. Several authors [1–7] have contributed significantly to the understanding of the degradation mechanisms of some organic pollutants in the bases of diagnosis and analysis in the gas and/or the liquid phases. Others, such as Yan et al. [8] have tried to understand the degradation pathway of AO7 dye in aqueous solution using analytical techniques such as GC–MS, ionic chromatography and UV/Vis spectroscopy. In this case, the hydroxyl radicals were presented as the only species responsible for the degradation of the dye molecules. These mechanisms do not take into account the mass transfer aspect between the plasma species and the treated liquid. It is for this reason that these mechanisms have long been controversies and remain relatively unidentified till now.

In the first part of this paper [9], three different model molecules were treated by the GAD process. The model molecules were chosen so that they differ according to their chemical structure, their air/water partitioning coefficient (Henry's constant k_H), and their reactivity with ozone. These molecules were 1-Heptanol ($k_H = 1{,}220$ w.u, low reactivity with ozone), phenol ($k_H = 70{,}644$ w.u, high reactivity with ozone), and para-chlorobenzoic acid, *p*CBA ($k_H \approx 200\,000$ w.u, low reactivity with ozone).The main conclusion was that the removal mechanisms differed depending on the characteristics of the molecule treated. Basing on experimental results, the following mechanisms were proposed:

1. Transfer from the liquid phase to the gas phase and reaction with gaseous short-lived species generated by the discharge in the case of 1-Heptanol (low solubility and low reactivity);
2. Degradation by $^{\cdot}OH$ radical in the liquid phase in the case of *p*CBA (high solubility and low reactivity);
3. Finally, in the case of phenol, the main degradation mechanism could be either its oxidation by ozone or its reaction with $NO_2^{\cdot}$ radicals produced by the dissociation of N_2O_4 in liquid phase.

In this second part, a numerical simulation coupling a simplified model describing the mass transfer at the gas–liquid interface, and a kinetic model with the main reactions in liquid and gas phases is proposed. The main objective of the modeling is to confirm or refute the degradation mechanisms proposed in the first part [9] for 1-Heptanol, phenol and *p*-chlorobenzoic acid.

Moreover, the simulation will allow to give estimations of the concentrations of the following short-lived species which are difficult to be measured using classical methods such as $^{\cdot}OH$ in the plasma plume and $NO_2^{\cdot}$. The concentration of peroxynitrous acid (ONOOH), long-lived species, was estimated in the aqueous phase before the beginning of the temporal post-discharge.

Methodology

Mass Transfer

The mass-transfer at the plasma-liquid interface was evaluated by mathematical simulations using COMSOL multiphysics 4.3.b version.

The Lewis and Whitman double film model [10] was used to describe the interaction phenomenology. According to this theory, the two phases are separated by an interface and a double film (one for each phase) adheres to this interface. The mass transfer takes place exclusively in this double stationary film by the molecular diffusion mechanism. In the bulk of each phase, the concentration of the solute is considered uniform due to a perfect mixing.

The thicknesses of the two films were calculated using experimental values of the overall mass transfer coefficients K_G and K_L are defined according to the following equations:

$$\Phi = K_G \times S \times \left(\frac{C_L}{He} - C_G\right) = K_L \times S \times (C_L - He \times C_G) \quad (1)$$

where Φ is the interfacial molar flow (mol s^{-1}), K_L overall mass transfer coefficient based on the liquid side (m s^{-1}), K_G overall mass transfer coefficient based on the gas side (m s^{-1}), C_L concentration of the solute in the liquid (mol m^{-3}), C_G concentration of the solute in the gas (mol m^{-3}), S gas–liquid interfacial area (m^2) and He Henry constant (mol m^{-1} Pas^{-1}).

The relations between overall mass transfer coefficient (K_G, K_L) and local mass transfer coefficient (k_G, k_L) are:

$$\frac{1}{K_G} = \frac{1}{k_G} + \frac{1}{He \times k_L} \quad (2)$$

For highly soluble compounds (He $\gg$ 0), we have $K_G = k_G$;

$$\frac{1}{K_L} = \frac{1}{k_L} + \frac{He}{k_G} \quad (3)$$

For poorly soluble compounds (He $\ll$ 0), we have $K_L = k_L$.

Two model organic compounds were chosen to determine experimentally the overall mass transfer coefficients: phenol as a soluble compound (He = 70,644 w.u [11]) and toluene as poorly soluble compound (He = 3.6 w.u [11]). To do that, the stripping of aqueous solutions of phenol and toluene (1 mmol L^{-1}) was carried out in the GAD reactor. The results are presented in Table 1.

The values presented confirm clearly the nature of the compounds used. The stripping of the soluble compound (phenol) is very difficult compared to that of the poorly soluble compound (toluene).

The mass balance performed in the liquid and gas phases of the two compounds, in a transient regime, gives local mass transfer coefficient values of: $k_L = 1.5 \times 10^{-4}$ m s^{-1} and $k_G = 0.11$ m s^{-1}.

Once k_G and $k_L$are known, the thicknesses of the two stationary films e_G and e_L respectively for gas and liquid, were calculated using the following equations:

$$e_G = \frac{D_G}{k_G} \quad (4)$$

$$e_L = \frac{D_L}{k_L} \quad (5)$$

Using $D_L = 10^{-9}$ m^2 s^{-1} and $D_G = 10^{-5}$ m^2 s^{-1} [10], the thicknesses are respectively $e_l = 10^{-6}$ m and e.g. $= 10^{-5}$ m.

Table 1 Phenol and toluene stripping

	Toluene	Phenol
Henry constant (WU*)	3.6 [11]	70,644 [11]
Stripping time (min)	4	90
Elimination (%)	20.6 ± 1.1	3.1 ± 0.2

* Without Unit

Kinetic Model

A simplified kinetic model was proposed to describe the plasma-chemical reactions taking place between (1) plasma species and (2) plasma species and pollutants. The reactions are presented in Table 2. All the kinetic constants were taken from the literature [11–25].

In general, the proposed mechanism is in agreement with the last study of the chemical proprieties of the GAD process realized by Brisset and Hnatiuc [12].

It is known that O_2, N_2 and H_2O are the main molecules present in humid air. These species are initially in their ground state. The power delivered by the electric source (900–1,200 watts) induces their excitation and ionization to form essentially $^{\cdot}OH$, $^{\cdot}NO$, O_3, NO_2, N_2O_3 and N_2O_4.

Hydroxyl radicals in the gas phase ($^{\cdot}OH^{(g)}$ with $He_1 = 760$) present in the plasma plume can be transferred in the liquid phase according to reaction (R1) to give $^{\cdot}OH^{(l)}$. Two hydroxyl radicals $^{\cdot}OH^{(l)}$ can react in the liquid phase to produce the H_2O_2 dimer hydrogen peroxide (R2).

The NO_x solubility in water varies typically in the following order $NO^{(g)} < NO_2^{(g)} < N_2O_4^{(g)}$ [11, 18, 19]. In our mechanism we assume that only $NO_2^{(g)}$ ($He_4 = 0.3$) and $N_2O_4^{(g)}$ ($He_5 = 39$) can be transferred in the liquid phase. The homolytic rupture of $N_2O_4^{(l)}$ in water can give two $NO_2^{\cdot(l)}$ according to reaction (R6). The reaction (R7) shows that the hydrolysis of $N_2O_4^{(l)}$ can also give nitrite and nitrate ions in the liquid phase. $NO_2^{-(l)}$ ions can react with $^{\cdot}OH^{(l)}$ to give more of $NO_2^{\cdot(l)}$ (reaction (R8)), and/or react with $O_3^{(l)}$ to product nitrate ions (reaction 10). The ozone molecule is poorly transferred from the plasma plume to the water according to its low Henry constant value ($He_9 = 0.3$). The NO_2 radicals produced by reactions (R6) and (R8) and reacting with $^{\cdot}OH^{(l)}$ give the peroxynitrous acid ONOOH (PON) according to reaction (R11).

Schwarz [25] has synthetized the pernitrous acid (or pernitric) acid by admixture of concentrated hydrogen peroxide and nitrogen pentoxide. Allen [26] has obtained the compound by bombardment of nitric acid with fast electrons. Halfpenny and Robinson [27] have attempted to obtain more information on the reaction between hydrogen peroxide and nitrous acid to determine the optimal conditions to synthesis the PON.

Since the plasma in humid air generates nitric acid, hydrogen peroxide and electrons, it is possible that the compound is formed in aqueous solution under specific conditions.

Peroxynitrous acid and its conjugate base peroxynitrite ($ONOO^-$) are the source of the temporal post-discharge phenomenon responsible for the degradation of the most organic pollutants in aqueous solutions [12]. The last plasma-chemical reaction (R12), in the absence of pollutant, indicates the PON transformation to NO_3^- which is more stable state for this molecule.

Pollutants can be oxidized according to their solubility in the liquid phase and/or in the gas phase. A global scheme of plasma-chemical reactions is proposed in Fig. 1. This kinetic model takes into account the affinities (rate constants) between plasma species

Table 2 Major plasma-chemical reactions

	Plasma-chemical reactions		Constant rates at 298 K	References
Distilled water	$^{\cdot}OH^{(g)} \xrightarrow{He_1} {}^{\cdot}OH^{(l)}$	R1	$He_1 = 760$	[11]
	$^{\cdot}OH^{(1)} + {}^{\cdot}OH^{(1)} \xrightarrow{k_2} H_2O_2^{(l)}$	R2	$k_2 = 10^7\ m^3\ mol^{-1}\ s^{-1}$	[12–17]
	$NO_2^{(g)} + NO_2^{(g)} \overset{k_3, k_{-3}}{\leftrightarrow} N_2O_4^{(g)}$	R3	$k_3 = 6.02 \times 10^6\ m^3\ mol^{-1}\ s^{-1}$ $k_{-3} = 4.4 \times 10^6\ m^3\ mol^{-1}\ s^{-1}$	[16]
	$NO_2^{(g)} \xrightarrow{He_4} NO_2^{(l)}$	R4	$He_4 = 0.3$	[11]
	$N_2O_4^{(g)} \xrightarrow{He_5} N_2O_4^{(l)}$	R5	$He_5 = 39$	[11]
	$N_2O_4^{(l)} \xrightarrow{He_5} NO_2^{(l)} + {}^{\cdot}NO_2^{(l)}$	R6	$k_6 = 7{,}10^3\ s^{-1}$ $k_{-6} = 4.5\ 10^5\ m^3\ mol^{-1}\ s^{-1}$	[17]
	$N_2O_4^{(l)} + H_2O \xrightarrow{k_7} NO_2^{-(l)} + 2H^+ + NO_3^{-(l)}$	R7	$k_7 = 10^6\ s^{-1}$	[17]
	$NO_2^{-(l)} + {}^{\cdot}OH^{(l)} \xrightarrow{k_8} NO_2^{(l)} + OH^-$	R8	$k_8 = 10^7\ m^3\ mol^{-1}\ s^{-1}$	[17, 18]
	$O_3^{(g)} \xrightarrow{He_9} O_3^{(l)}$	R9	$He_9 = 0.3$	[11]
	$NO_2^{-(l)} + O_3^{(l)} \xrightarrow{k_{10}} NO_3^{(l)} + O_2$	R10	$k_{10} = 5.8 \times 10^2\ m^3\ mol^{-1}\ s^{-1}$	[17, 18]
	$NO_2^{(l)} + {}^{\cdot}OH^{(l)} \xrightarrow{k_{11}} HOONO^{(l)}$	R11	$k_{11} = 1.2 \times 10^7\ m^3\ mol^{-1}\ s^{-1}$	[19]
	$HOONO^{(l)} \xrightarrow{k_{12}} NO_3^- + H^+$	R12	$k_{12} = 1.1\ s^{-1}$	[20]
1-Heptanol	$C_7H_{16}O^{(l)} \xrightarrow{He_{13}} C_7H_{16}O^{(g)}$	R13	$He_{13} = 1{,}220$	[11]
	$C_7H_{16}O^{(g)} + {}^{\cdot}OH^{(g)} \xrightarrow{k_{14}} Products$	R14	$k_{14} = 5.1 \times 10^6\ m^3\ mol^{-1}s^{-1}$	[21]
	$C_7H_{16}O^{(1)} + {}^{\cdot}OH^{(1)} \xrightarrow{k_{15}} Product$	R15	$k_{15} = 7.4 \times 10^6\ m^3\ mol^{-1}s^{-1}$	[22]
Phenol	$C_6H_6O^{(l)} \xrightarrow{He_{16}} C_6H_6O^{(g)}$	R16	$He_{16} = 70{,}644$	[11]
	$C_6H_6O^{(l)} + {}^{\cdot}OH^{(l)} \xrightarrow{k_{17}} Products$	R17	$k_{17} = 10^7\ m^3\ mol^{-1}s^{-1}$	[23]
	$C_6H_6O^{(l)} + NO_2^{(l)} \xrightarrow{k_{18}} Products$	R18	$k_{18} = 10^6\ m^3\ mol^{-1}s^{-1}$	[24]
	$C_6H_6O^{(l)} + HOONO \xrightarrow{k_{19}} Products$	R19	$k_{19} = 1.25\ m^3\ mol^{-1}\ s^{-1}$	[24, 25]
	$C_6H_6O^{(l)} + O_3^{(l)} \xrightarrow{k_{20}} Products$	R20	$k_{20} = 10^3\ m^3\ mol^{-1}\ s^{-1}$	
*p*CBA	$pCBA^{(l)} \xrightarrow{He_{21}} pCBA^{(g)}$	R21	$He_{21} = 400{,}000$*	[11]
	$pCBA^{(l)} + O_3^{(l)} \xrightarrow{k_{22}} Products$	R22	$k_{22} = 5 \times 10^9\ m^3\ mol^{-1}s^{-1}$	[24, 25]
	$pCBA^{(l)} + {}^{\cdot}OH^{(l)} \xrightarrow{k_{23}} Products$	R23	$k_{23} = 5.2 \times 10^6\ m^3\ mol^{-1}s^{-1}$	[24, 25]

* *p*CBA Henry's constant is bibliographically unknown. In this work, it was replaced by the one of benzoic acid whose chemical structure is similar to *p*CBA molecule

and/or of pollutant models and their solubilities (Henry's constants). In the case of 1-Heptanol, phenol and *p*CBA, the mechanism is express as follows:

1. 1-Heptanol: very volatile (R13), the pollutant is mainly stripped in the gas phase where it reacts with $^{\cdot}OH^{(g)}$ as it is shown in reaction (R14). Some residual molecules of 1-Heptanol can also react with $^{\cdot}OH^{(l)}$ in water (R15);
2. Phenol: moderately volatile, the phenol reacts with $^{\cdot}OH^{(l)}$ (R17), $NO_2^{(l)}$ (R18), PON (R19) and O_3 (R20);

3. *p*CBA: very soluble, it reacts with $O_3^{(l)}$ and $^{\cdot}OH^{(l)}$ according to reactions (22) and (23), respectively.

Modeling

Geometry

In the zone near of the gas–liquid interface there is a symmetric gas flow. This has allowed us to simplify the 3D configuration into a 1D configuration. The latter geometric model was used to study the reactive transfer of plasma active species and pollutants in the GAD reactor.

The 1D representing the GAD reactor shown in Fig. 2 includes four distinct domains:

1. Domain (1): plasma phase perfectly homogenized. Its length is of 0.06 m. This dimension is in related to the void volume of the reactor occupied by the plasma;
2. Domain (2): gas film with a thickness e.g. of 10^{-4} m (estimated by the Eq. 4);
3. Domain (3): liquid film with a thickness e_l of 10^{-5} m (estimated by the Eq. 5);
4. Domain (4): perfectly homogenized liquid phase with a length of 0.07 m corresponding to the height of the liquid volume in the reactor.

Special Material Balance

The 'convection–diffusion' Eq. [10] was solved for each species in the 4 domains using Comsolmultiphysics commercial software:

$$\frac{\partial C_i}{\partial t} - D_i \times \frac{\partial^2 C_i}{\partial x^2} + u \times \frac{\partial C_i}{\partial x} = R_i \tag{6}$$

where C_i is the concentration of species i (mol m^{-3}); D_i is the diffusion coefficient of the species i in the domain (m^2 s^{-1}); u is the fluid velocity in the domain (m s^{-1}) and R_i is the source term representing the production and/or consumption of species i due to chemical reactions (mol m^{-3} s^{-1}).

In the domains (2) and (3), the transfer occurs only by diffusion with $D_L = 10^{-9}$ m^2 s^{-1} and $D_G = 10^{-5}$ m^2 s^{-1}. There is no convection (u = 0).

In the domains (1) and (4), the gas and liquid phases are considered as perfectly stirred thanks to the convection. Since the velocity of the fluid (u) is unknown, it has been fixed at 0 and we have affected high values to the diffusion coefficient which becomes an apparent diffusion coefficient: $D_{app,G} = 10^{-1}$ m^2 s^{-1} and $D_{app,L} = 10^{-3}$ m^2 s^{-1}.

The boundary conditions are given as follows:

1. 1 At the gas–liquid interface (between domains 2 and 3), there is a thermodynamic equilibrium between the gas phase and the liquid phase. The equilibrium is expressed by Henry's law:

$$C^{(l)} = C^{(g)} \times He \tag{7}$$

where C_L and C_G (mol m^{-3}) are the concentrations of the species in the liquid and gas phases, respectively. He (WU) is the Henry constant of the species.

The molar flux density across the gas–liquid interface is calculated using Fick law:

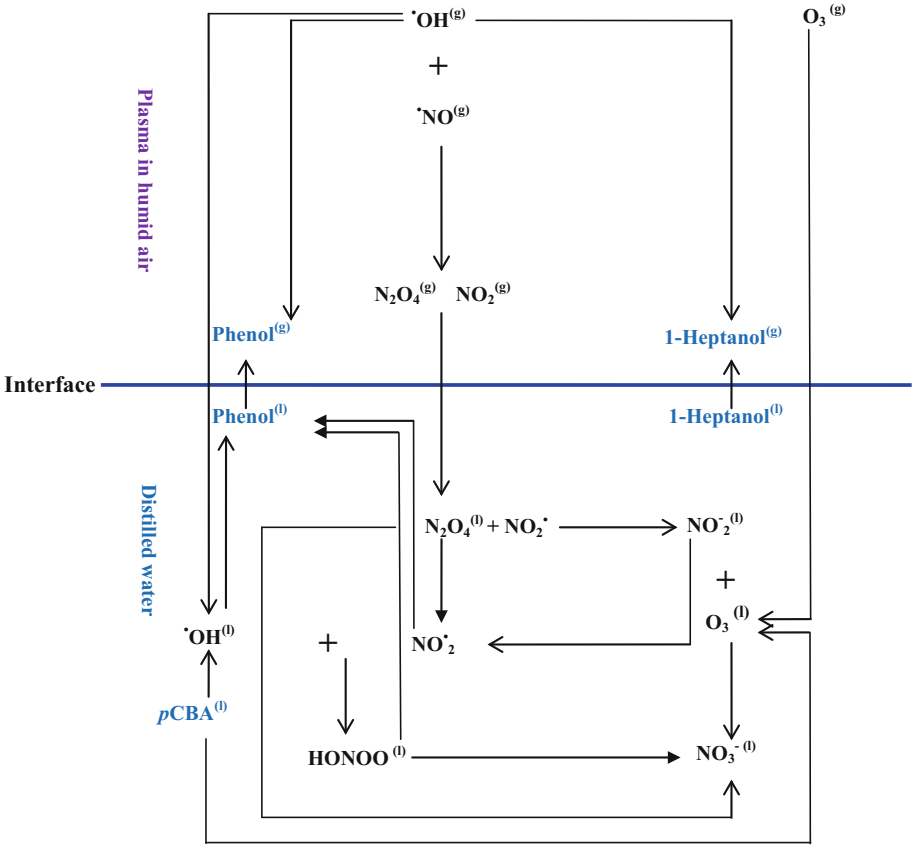

Fig. 1 A proposed global scheme of plasma-chemical reactions

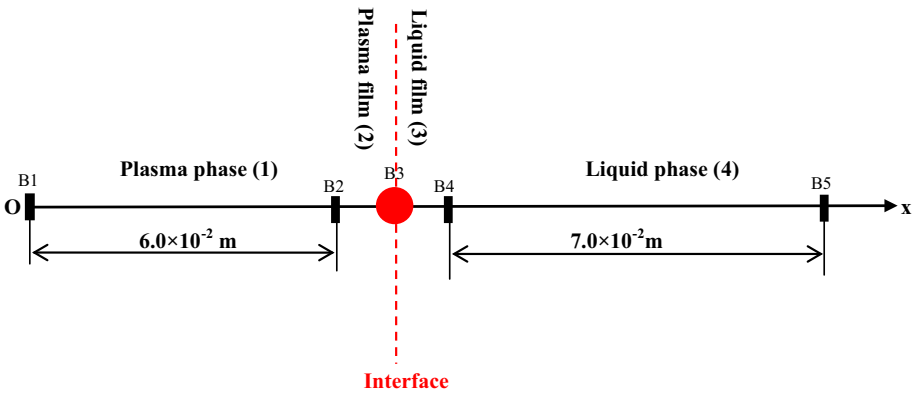

Fig. 2 GAD reactor 1D geometry

$$J(\text{molm}^{-2}\text{s}^{-1}) = -D_G \times \text{grad}(C_i^{gas}) \quad (8)$$

2. At boundaries B2 and B4, the continuity boundary condition was considered.
3. At boundary B5, a zero flux (0) was considered due to the presence of a wall (bottom of the reactor).
4. At boundary B1 the extremity of the segment (top side) representing the gaseous phase (domain 1), we have introduced an expression of the molar flow (in mol m^{-2} s^{-1}) from the mass balance in the gas phase:

$$\text{Flux} = \frac{Q}{S} \times (C^{in} - C^{out}) \quad (9)$$

With $Q = 0.22 \times 10^{-3}$ m^3 s^{-1} is the gas flow rate, $S = 63.5 \times 10^{-4}$ m^2 is the section of the cylindrical GAD reactor and C^{in}, C^{out} are the concentration of species in the extremities of the domain 1.

The NO_2 and O_3 concentrations obtained experimentally [9] in the plasma plumewere of 0.0570 and 0.0246 mol m^{-3}, respectively. These values were maintained constants in the Eq. (6). However, the OH radical which the concentration is difficult to measure was fitted at 0, 4, 12, 24, 100 and 250 ppm to verify the validity of the proposed model.

Results and Discussion

Plasma Species Quantification Without Pollutants

The concentration of H_2O_2, $NO_2^{\cdot}$, NO_2^-, NO_3^- and PON (ONOOH) species in distilled water exposed to the plasma plume during 1,800 s are calculated from the kinetic model (Eq. 6) by introducing Reactions (R1–R12).

To establish the mass balance of these species, it is necessary to know the concentration of OH radicals produced by the GAD in the gas phase.These radicals are the precursor of major plasma reactions generated by GAD in humid air. For this reason, its concentration in the gas phase will be varied to fit the experimental data to the kinetic model. Bruggeman and Schram [28] have shown that $^{\cdot}OH^{(g)}$ density in the plasma plume is 10^{20} cm^{-3} corresponding to a concentration of 4 ppm.

Figures 3 and 4 show the calculated concentrations of NO_2^-, NO_3^-, H_2O_2, $NO_2^{\cdot}$, and ONOOH (PON) for 0, 4, 12, 24, 100 and 250 ppm of $^{\cdot}OH^{(g)}$.

Nitrate ions and hydrogen peroxide are the most stable plasma species in the liquid phase, since their atoms are in their highest oxidation state. Experimentally, we have obtained 5.62 and 0.02 mol $m^{-3}$of NO_3^- and H_2O_2 concentrations, respectively. By calculating at 1,800 s and a fitted $^{\cdot}OH^{(g)}$ concentration at 250 ppm, the $NO_3^-$and H_2O_2 concentrations were of 5.09 and 1.21 mol m^{-3}, respectively. When $[^{\cdot}OH^{(g)}] = 100$ ppm, these values were of 2.31 for NO_3^- and 0.134 mol m^{-3} for H_2O_2. In this case, the nitric ions are in the same range of magnitude of experimentally data [9] due to the NO_2^- ions transfer in the liquid phase. This transfer is chemically accelerated in the presence of high concentration of OH radicals to give stable nitric species such as NO_3^-. Once the latter is formed, the excess of OH radicals are recombined to give more of H_2O_2 species. Indeed, for $[^{\cdot}OH^{(g)}] > 100$ ppm, especially for 24 ppm, the NO_3^- concentration was of 0.106 mol m^{-3} which is relatively far from experimental results [9], due to the insufficient

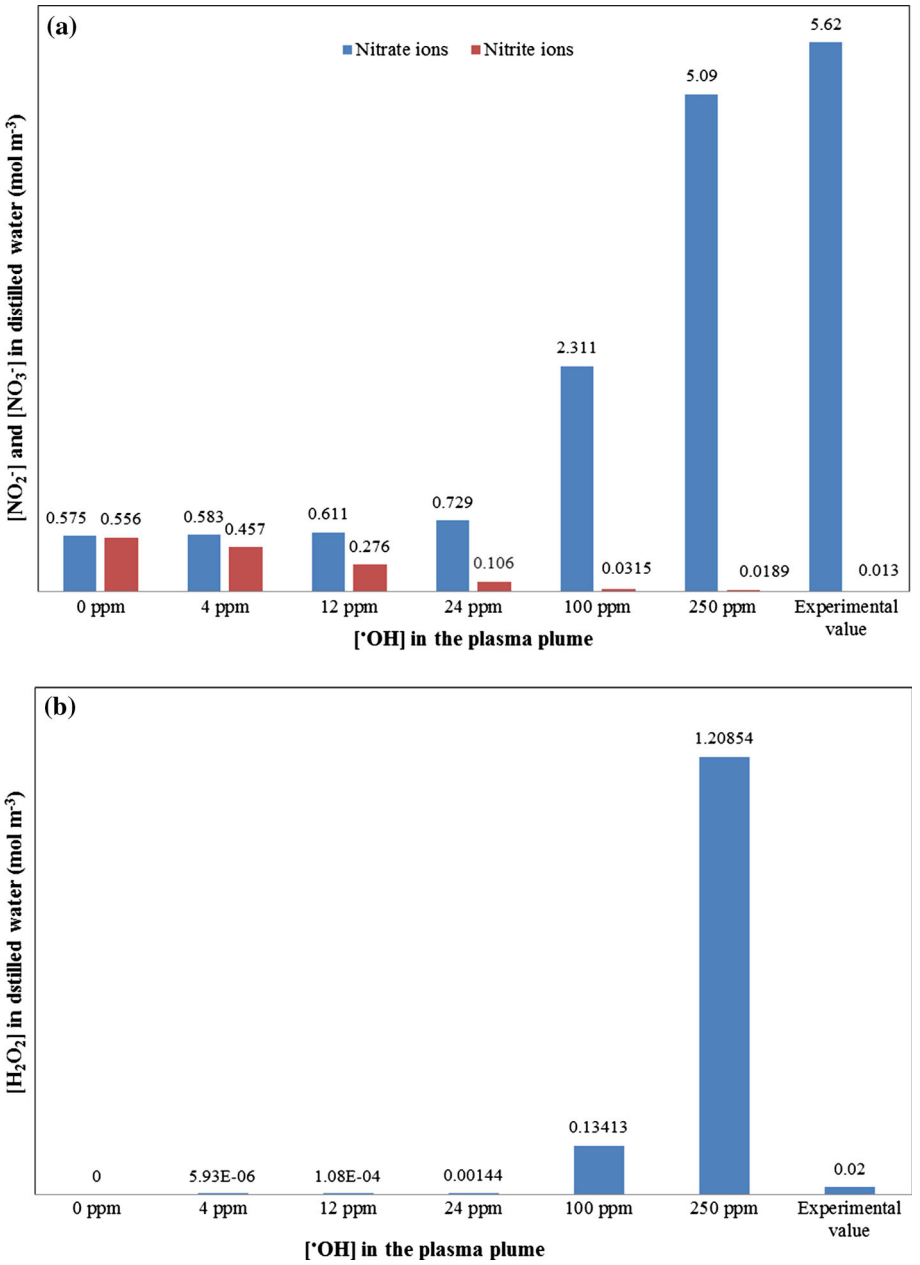

Fig. 3 Plasma species produced in distilled water during 1,800 s for [$^{\cdot}OH^{(g)}$] = 0, 4, 12, 100 and 250 ppm: **a** NO_2^- and NO_3^-, **b** H_2O_2

of $^{\cdot}OH$ able to oxidize the reduced forms of NO_x. However, the H_2O_2 concentration was of 0.0014 mol m^{-3} which is an acceptable value compared to the one calculated for 100 and 250 ppm of OH radicals. The concentration of H_2O_2 can be the subject of many

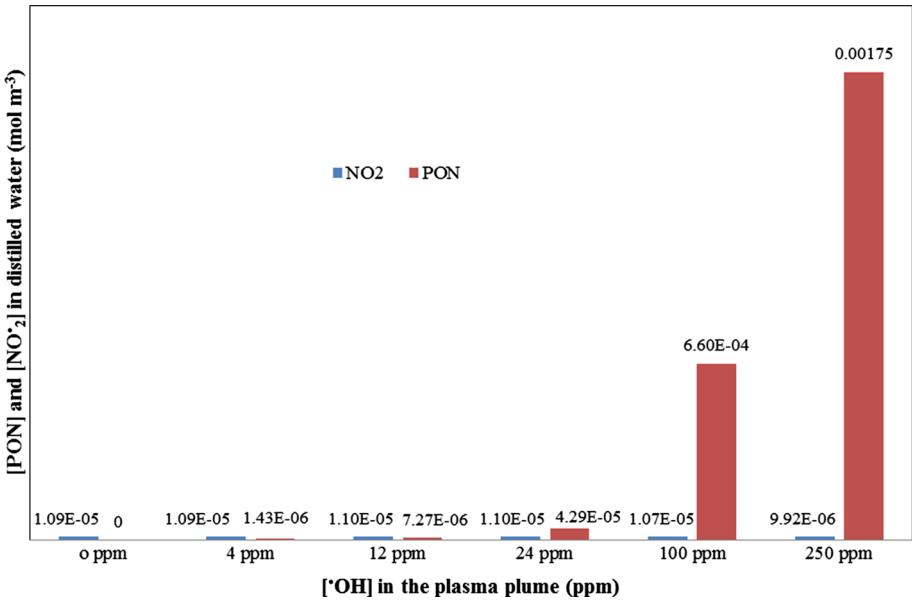

Fig. 4 Plasma species produced in distilled water during 1,800 s for [$^{\cdot}OH^{(g)}$] = 0, 4, 12, 100 and 250 ppm: $NO_2^{\cdot}$ and HONOO

interpretations since our mechanism does not take into account their dissociation to OH radicals by UV rays emitted by GAD [29], and also their stripping from the liquid to the plasma phase.

The oxidation of nitrite ions by $OH^{(l)}$ radicals gives NO_2 radicals ($NO_2^{\cdot}$) (reaction 8) which is responsible for the formation of PON species (reaction (R11)). Currently, it is impossible to determinate experimentally the PON and $NO_2^{\cdot}$ concentrations in aqueous solution. By simulation it was possible to calculate them at 1,800 s and for different concentration of $^{\cdot}OH^{(l)}$.

Without OH radicals transfer in water (R1), the concentration of PON and $NO_2^{\cdot}$ are zero and 1.09×10^{-5} mol m^{-3}, respectively. The presence of NO_2 radicals in this case is mainly attributed to the N_2O_4 present in water. Concerning the PON specie, we know that $^{\cdot}OH^{(l)}$ is the precursor of HOONO according to reaction (R11), so without hydroxyl radicals it is impossible to form peroxynitrous acid in aqueous media.

At low OH radical concentrations (4–24 ppm), the [PON] changes from 1.43×10^{-6} to 4.29×10^{-5} mol m^{-3} while the [$NO_2^{\cdot}$] is of 1.1×10^{-5} mol m^{-3}. At high OH radical concentrations (100–250 ppm) the NO_2 radical concentrations is situated between 9.92×10^{-6} and 1.07×10^{-5} mol m^{-3} with an important increase of PON concentration which attained 6.6×10^{-4} and 1.75×10^{-3} mol m^{-3} for 100 and 250 ppm, respectively. This can be checked by the reaction (R10) which clearly states that the concentration HOONO increases with the $^{\cdot}OH$ transferred in the water. The PON species is more stable than the NO_2 radical; it is responsible for the temporal post-discharge of plasma generated in GAD humid air. The calculating of its lifetime in aqueous solution have given 23.6 h, time taken to degrade Alizarine red S anthraquinonic dye in the same conditions according to the works done by Merouani et al. [30].

Mechanism Degradation

Plasma-chemical reactions presented in Table 2, were introduced in the model to study the mechanism of degradation of the three pollutant models (1 mol m^{-3}). The strategy is to fit different values of $^{\cdot}OH^{(g)}$ concentrations in order to reach the experimental degradation rate.

1-Heptanol

Figure 5 presents the variation of 1-Heptanol degradation versus the treatment time for different $^{\cdot}OH^{(g)}$ radical concentrations.

In absence of $^{\cdot}OH^{(g)}$, the calculation shows that 44 % of 1-Heptanol is eliminated; however, in the experiment study 24 % were stripped by humid air. The difference can be explained by the existence of systematic errors during analysis and/or the limits of the kinetic model.

The 1-Heptanol degradation process increases with OH concentration: for 12, 24, 40 and 100 of $^{\cdot}OH^{(g)}$ concentrations, the degradation rate was of 70, 84, 87 and 93 %, respectively. A slowdown degradation phenomenon is observed when the $^{\cdot}OH^{(g)}$ concentration reached 100 ppm. This result can be explained limiting step due to the transfer of OH radicals from plasma to liquid phase.

The degradation rate obtained experimentally was of 93 %, which is in agreement with the calculated value for $^{\cdot}OH^{(g)}$ concentration fitted at 100 ppm. It should be noted that the other concentrations of OH radicals lead to degradation rates relatively close to the experimental one, especially for $[^{\cdot}OH^{(g)}]$ of 24 and 40 ppm.

The fraction of 1-Heptanol degraded in the gas phase was of 82 % for $[^{\cdot}OH^{(g)}] =$ 24 ppm. In this case, the calculated degradation rate is in agreement with the experimental one, we can suppose that the removal of the molecule takes place essentially in the gas phase.

Franclemont et al. [31] have recently demonstrated that the degradation of volatile compounds occurs in the gas phase during the treatment of water by a Pulsed Electrical Discharge. They have also assumed that the more the diffusion of these compounds is important the more the degradation is pronounced.

Phenol

Figure 6 depicts the variation of the phenol degradation versus time, at fixed concentrations of $^{\cdot}OH^{(g)}$. When the latter was fitted at 0 ppm, the degradation rate was 78 % after 1,800 s. The absence of OH radicals in the aqueous solution does not compromise the removal of phenol. In this case, the degradation is due to the presence of NO_2 radicals in the solution according to reaction (R18). The degradation takes place essentially in the liquid phase since the stripping rate of phenol is 3.1 % only in the gas phase. The experiments [9] have demonstrated by GC–MS analysis the formation of the Nitrophenol compound during the plasma-GAD treatment. The simulations suggest the formation of the same organic compound according to reaction (R18).

The $^{\cdot}OH^{(g)}$ concentrations were fitted at 12, 24 and 40 ppm to evaluate their contribution on the phenol degradation rate which were of 93, 94 and 98 %, respectively for 1,800 s. The experiments [9] have given 100 % for 700 s of plasma treatment time. The difference can be explained by the fact that OH radicals can attack the phenol molecule according to reaction (R17) and/or it can react preferentially with NO_2 radicals to form

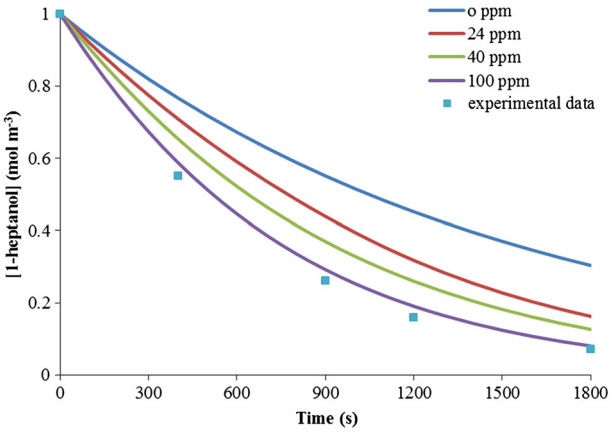

Fig. 5 1-Heptanol removal in liquid phase versus time for different [$^{\cdot}OH^{(g)}$]

HOONO (R11). This species may react with the pollutant according to (R17). However, the high acidity of the media after 1,800 s of treatment (pH < 2.1) can modify the kinetic of the reaction (R19): protonation of the media will stabilise the PON and will increase the life time of this species. Consequentially, the kinetic constant of the reaction (R19) will be greater than 1.25 m^3 mol^{-1} s^{-1}, which can reduce the reaction time to 700 s instead of 1,800 s. In this context, Keith and Powell [32] have proposed for the acid-catalyzed decomposition of ONOOH the following mechanism:

$$ONOOH \overset{Ka}{\longleftrightarrow} ONOO^- + H^+ \quad (R24)$$

$$ONOOH \overset{k_{HA}}{\longleftrightarrow} NO_3^- + H^+ \quad (R25)$$

According to this scheme, the apparent rate constant of PON decomposition k is obtained by the following equation [21]:

$$k = \frac{k_{HA} \times [H^+]}{K_a + [H^+]} \quad (10)$$

where k_{HA} is the pH-dependent rate constant.

Peroxynitrite is relatively stable in alkaline solution. However, at neutral or acidic pH it decomposes fast. The absorbance at 302 nm then decreases following an exponential function [33]. The rate constant of peroxynitrite decomposition at pH 7.4 is 0.26 s^{-1} at 25 °C and 0.9 s^{-1} at 37 °C [33, 34].

The pH dependence alone, does not explain the difference between the two rate constants. Probably, there is a competition between the phenol and its by-products degradation in their reaction with PON plasma species. Daiber et al. [18] have demonstrated that by-products such as: hydroxyphenols, catechol, *p*-benzoquinone, 4-nitrosophenol, and bis phenols can also react with PON. The kinetic model does not take into account the competition reactions.

The contribution of ozone species in the degradation of phenol is very small; indeed, by calculating we found just 1.3 % of degradation rate affected to the presence of O_3 species. This can be explained by the poor transfer of O_3 in the liquid phase and the low desorption of phenol from liquid to plasma plume. Other plasma-species contribute to the degradation

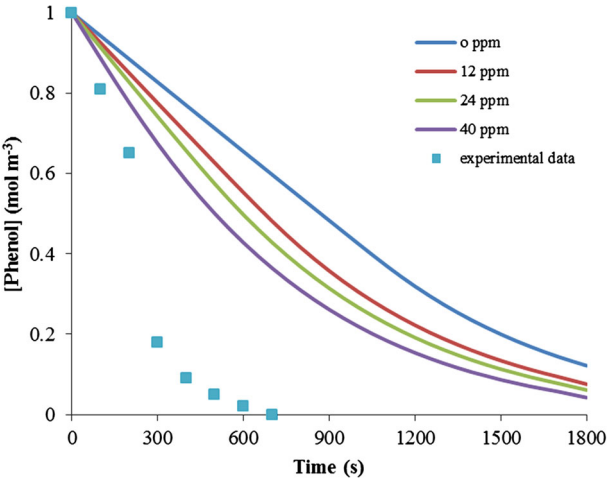

Fig. 6 Phenol removal in liquid phase versus time for different [$^{\cdot}OH^{(g)}$]

of phenol more efficiently: $^{\cdot}OH$ with 13.7 %, $NO_2^{\cdot}$ with 72 % and the PON with 13 %. When the discharge is stopped, the PON, long-lived plasma-species, will continue to react with the molecule of phenol in post-discharge step.

pCBA

In the case of *p*CBA, experimental results showed that the degradation takes place in the liquid phase. OH radicals and ozone may be responsible for the oxidation of the *p*CBA according to (R22) and (R23), respectively.

Figure 7 shows the *p*CBA concentration versus time and different $^{\cdot}OH$ concentrations. When [$^{\cdot}OH^{(g)}$] = 0, no degradation was observed for the pollutant. The fitting at 12, 24 and 40 ppm of OH radicals give respectively 8, 19 and 40 % of degradation rates for 1,800 s. Experimentally, it was 19 % which is in agreement with the calculating for an $^{\cdot}OH$ concentration of 24 ppm.

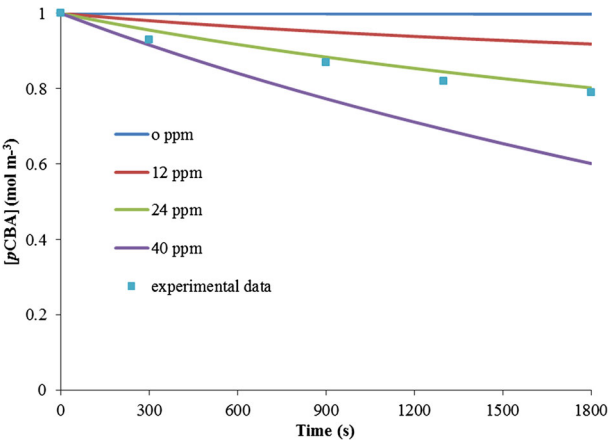

Fig. 7 *p*CBA removal in liquid phase versus time for different [$^{\cdot}OH^{(g)}$]

Although the *p*CBA is very reactive with ozone (R22), its degradation is due only to the short-lived plasma species such as OH radicals, because O_3 is weakly transferred in the solution ($He_9 = 0.3$). The contribution of ozone to degrade the *p*CBA molecule is of 1.8 % according to the calculation. The same explanation was given by Beltran-Heredia et al. [35] when they compare the degradation of *p*CBA in aqueous solution by several oxidation processes: the low solubility of ozone in water and the limitations of mass transfer from gas to liquid suggest that $^{\cdot}OH$ is only specie responsible for the degradation of *p*-hydroxybenzoic acid.

Conclusion

In the first part of this work, three different kind of organic pollutants were degraded by plasma-Glidarc process. The selected pollutant models were: 1-Heptanol, phenol and *p*CBA in aqueous medium. The study showed that the degradation mechanism by Glidarc depends on the solubility/volatility ratio of the compounds.

In this part, a kinetic modeling approach was used to describe the plasma-treatment of the three organic compounds. Simulations based on the diffusion–convection–reaction model were applied under COMSOL software multiphysics 4.3.b version. The calculations were based on the results obtained in the first part of this paper in order to have outputs relatively similar to reality. The strategy was to fit the concentration of the plasma-species so as to get the experimental degradation rate values.

A simplified 1D geometric model was used to describe the reactions involving the active plasma-species and the three pollutants. The results are presented as follows:

1. 1-Heptanol is degraded by a stripping assisted by plasma-chemical reactions in the gas phase with hydroxyl radicals;
2. Phenol is degraded in the liquid phase by: $NO_2^{\cdot}$, $^{\cdot}OH$ and HOONO;
3. *p*CBA is degraded in the liquid phase only by $^{\cdot}OH$;
4. In view of the calculation results, the concentration of OH radicals in the plasma plume is apparently of the order of 24 ppm, coherent with the experimental measurements available in the literature [28]. The $NO_2^{\cdot}$ in water is principally coming from N_2O_4, its concentration is of 1.1×10^{-5} mol m^{-3}. In this case the concentration of HOONO, species formed from NO_2 and OH radicals, will be equal to 4.29×10^{-5} mol m^{-3} in the liquid phase.

Generally, this study has proved the specific role of the main plasma-species in the degradation of organic pollutants. Other investigations are in progress to improve the modeling of the phenomenon by taking into account plasma reactions between the active species and the by-products degradation.

Acknowledgments The authors thank 'Erasmus Mundus' and 'Pierre et Marie Curie University' for their financial help during Mr. Ghezzar post-doctoral fellowship.

References

1. Locke BR, Thagard SM (2009) IEEE Trans Plasma Sci 37(4):494–501
2. Pascal S, Moussa D, Hnatiuc E, Brisset JL (2010) J Hazard Mater 175:1037–1041
3. Locke BR, Thagard SM (2012) Plasma Chem Plasma Process 32:875–917
4. Benstaali B, Boubert P, Cheron BG, Addou A, Brisset JL (2002) Plasma Chem Plasma Proc 22:553–571

5. Moussa D, Brisset JL (2003) J Hazard Mater 102:189–200
6. Abdelmalek F, Toress RA, Combet E, Petrier C, Pulgarin C, Addou A (2008) Sep Purif Technol 63:30–37
7. Burlica R, Kirkpatrick MJ, Finney WC, Clark RJ, Locke BR (2004) J Electrostat 62:309–321
8. Yan JH, Liu YN, Bo Z, Li X, Den KF (2008) J Hazard Mater 157:441–447
9. Iya-Sou D, Laminsi S, Cavadias S, Ognier S (2013) Plasma Chem Plasma Process 33:97–113
10. Bird BR, Stewart WE, Light foot EN (2007) Transport phenomena. Wiley, New York
11. Sander R, Air Chemistry Department, http://www.mpch-mainz.mpg.de/~sander/res/henry.html. Accessed 8 April 1999
12. Brisset JL, Hnatiuc E (2012) Plasma Chem Plasma Process 32:655–674
13. Bo Z, Yan J, Li X, Chi Y, Cen K (2009) J Hazard Mater 166:1210–1216
14. Buxton GV, Greenstock CL, Helman WP, Ross AB (1988) J Phys Chem Ref Data 17:513–886
15. Patwardhan JA, Joshi JB (2003) AIChE J 49:2728–2748
16. Radi R, Denicola A, Alvarez B, Ferrer-Sueta G, Rubbo H (2000) In: Chapter 4 Nitric oxide: biology and pathobiology. Academic Press, Waltham
17. Vione D, Maurino V, Minero C, Pelizzeti E (2001) Chemosphere 45:903–910
18. Daiber A, Mehl M, Ullrich V (1998) Nitric Oxide Biol Chem 2:259–269
19. Koppenol WH, Moreno JJ, Pryor WA, Ischiropoulos H, Beckman JS (1992) Chem Res Toxicol 5:834–842
20. Atkinson R, Baulch D, Cox R, Hampson R, Kerr J, Troe J (1992) J PhysChem Ref Data 21:551–562
21. Sweeney AJ, Liu YA (2001) Ind Eng Chem Res 40:2618–2627
22. Kohnen LS, Mouithys-Mickalad A, Deby-Dupont G, Deby T, Hans P, Lamy M, Noelsa A (2003) Nitric Oxide 8:170–181
23. Zhang Y, Zhou L, Zeng C, Wang Q, Wanga Z, Gao SA, Ji Y, Yang X (2013) Chemosphere 93:1747–1754
24. Azrague K, Osterhus SW, Biomorgi JG (2009) Water Sci Technol 59:1209–12017
25. Schwarz Z (1948) anorg Chem 1:256
26. Allen N (1948) J Phys Coll Chem 52:479
27. Halfpenny E, Robinson PL (1952) J Chem Soc 168:928–938
28. Bruggeman P, Schram DC (2010) Plasma Sources Sci Technol 19:1–9
29. Moreau M, Orange N, Feuilloley MGJ (2008) Biotechnol Adv 26:610–617
30. Merouani DR, Abdelmalek F, Ghezzar MR, Semmoud A, Addou A, Brisset JL (2013) Ind Eng Chem Res 52(4):1471–1480
31. Franclemont J, Mededovic Thagard S (2014) Plasma Chem Plasma Process 34:705–719
32. Keith WG, Powell E (1969) J Chem Soc A 90–90
33. Warman P (1998) In: Alfassi Z (ed) N centered radicals, Chap. 5. Wiley, Chichester, pp 155–180
34. Radi R (1998) Chem Res Toxicol 11:720–721
35. Beltran-Heredia J, Torregrosa J, Dominguez JR, Peres JA (2001) Chemosphere 42:351–359